INTERNATIONAL JOURNAL OF HYDROGEN ENERGY 37 (2012) 8490–8498

Available online at www.sciencedirect.com

SciVerse ScienceDirect

journal homepage: www.elsevier.com/locate/he

Numerical model of a thermoelectric generator with compact plate-fin heat exchanger for high temperature PEM fuel cell exhaust heat recovery

Xin Gao, Søren Juhl Andreasen, Min Chen, Søren Knudsen Kær*

Department of Energy Technology, Aalborg University, Pontoppidanstræde 101, Aalborg DK-9220, Denmark

ARTICLE INFO

Article history:
Received 25 December 2011
Received in revised form
22 February 2012
Accepted 4 March 2012
Available online 28 March 2012

Keywords:
Thermoelectric generator
Heat recovery
Fuel cell
Discretized model
Heat exchanger database

ABSTRACT

This paper presents a numerical model of an exhaust heat recovery system for a high temperature polymer electrolyte membrane fuel cell (HTPEMFC) stack. The system is designed as thermoelectric generators (TEGs) sandwiched in the walls of a compact plate-fin heat exchanger. Its model is based on a finite-element approach. On each discretized segment, fluid properties, heat transfer process and TEG performance are locally calculated for higher model precision. To benefit both the system design and fabrication, the way to model TEG modules is herein reconsidered; a database of commercialized compact plate-fin heat exchangers is adopted. Then the model is validated against experimental data and the main variables are identified by means of a sensitivity analysis. Finally, the system configuration is optimized for recovering heat from the exhaust gas. The results exhibit the crucial importance of the model accuracy and the optimization on system configuration. Future studies will concentrate on heat exchanger structures.

1. Introduction

With the diminishing reserve of fossil fuels and the rising concern on global green-house gas emissions, more attention is being drawn by fuel cells [1]. Among other fuel cell technologies, high temperature polymer electrolyte membrane fuel cell (HTPEMFC) power systems are considered to be promising in practice [2]. Due to the high operating temperatures of HTPEMFCs (160°C–180 °C), the waste heat is of high quality and thermoelectric generators (TEGs) are introduced herein to recover this exhaust heat for electricity. As electric power generators, TEGs are advantageous in low grade heat recovery [3]. As opposed to traditional energy conversion devices, they have very simple structures and no moving parts. In addition, they are environmentally friendly, silent, reliable, exhibit excellent scalability and pure DC power output. Currently, TEGs are restricted to low heat-to-power conversion ratios. They are primarily competitive in niche applications, such as exhaust heat recovery, remote power supply and back-up power units [4,5]. If their efficiency can be improved in the future, for example from the present device figure of merit (ZT) $\approx$ 1 to ZT $\geq$ 2, many applications will materialize [6,7]. More widespread use of thermoelectrics requires not only novel materials with improved performance characteristics [8–10], but also TEG systems properly constructed [11–13].

Research on TEG systems can be categorized into optimization of the TEG modules themselves, and assembly of TEG modules with heat transfer structures. There are numerous publications considering the inner structure of TEG modules [14–17]. However, as mentioned by Hendricks and Lustbader [18], the whole TEG system should be studied as an integrated

* *Corresponding author*. Tel.: +45 21370579, fax: +45 98151411.
E-mail addresses: xga@et.aau.dk (X. Gao), skk@et.aau.dk (S.K. Kær).
0360-3199/$ – see front matter
doi:10.1016/j.ijhydene.2012.03.009

solution, because TE material properties and heat exchanging performance are tightly intertwined. Modeling and simulation plays the main role in the studies referenced in the next section.

Much effort has been made to study a single-/multi-element TEG module with its external heat reservoirs [19–21]. However, in practice, a concrete TEG system is always a combination of TEG modules with proper heat exchanging structures in very large scale installations to duly account for the magnitude of the exhaust heat sources. Suzuki and Tanaka compared the performance of 15 flat thermoelectric panels [22] and 6 different geometrical arrangements of cylindrical thermoelectric tubes [23]. Crane and Jackson [24] proposed a numerical model of a practical TEG waste heat recovery system with an advanced cross-flow heat exchanger and later the model was validated in experiments. Based on the aforementioned research work, Yu and Zhao [25], Smith [26] and Espinosa et al. [27] used different numerical models in a TEG system investigation for different waste heat sources. Recovering exhaust heat from fuel cells is a relatively novel application of TEGs. Chen et al. [28] proposed a module-level three dimensional TEG model in ANSYS FLUENT for the convenience of the co-design and co-optimization of a PEMFC-TEG system. The PEMFC-TEG system was also preliminarily demonstrated in the lab. A solid oxide fuel cell-TEG (SOFC-TEG) hybrid system was optimized on the main variables and the operating conditions in [29] using a zero-dimensional system model. Overall, the previous work has significant attributes in analyzing TEGs in practical applications. Some features can be further enhanced, including the following:

1) Fluid properties, flow condition, heat transfer [20] and TEG performance are locally resolved on each segment in a discretized TEG heat recovery system model for higher model accuracy.
2) The recovery system model is engineering-oriented. Factors affecting the system performance are able to be co-optimized in the model.
3) Mature heat exchanger structures and commercially available TEG modules are used in the model to benefit the system optimization and fabrication.

In the present paper, a TEG exhaust heat recovery system is modeled and optimized for the cathode exhaust gas of a HTPEMFC stack. Basically, it is a system similar to compact plate-fin heat exchangers but with TEG modules mounted on the walls. Cathode exhaust gas and coolant water are the working media. A numerical model for the system is proposed and validated. The model is intended to optimize the system design and operation with higher accuracy and flexibility as well as to assist the system fabrication. Sensitivity analyses are then carried out to identify the parameter priority for later configuration optimization. Finally, the system configuration is optimized.

2. Model description

The chosen architecture of the TEG exhaust heat recovery system is illustrated in Fig. 1. The compact heat exchanger housing is placed in the middle for the exhaust gas. Two aluminum blocks are settled at the top and the bottom.

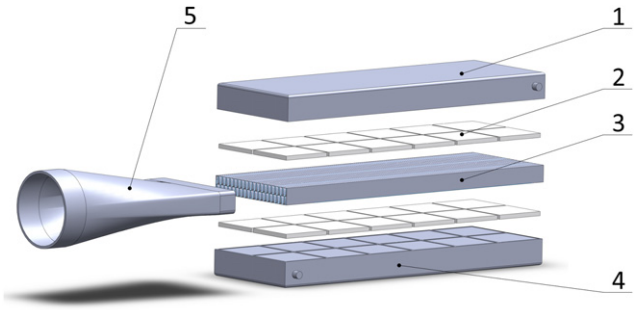

Fig. 1 – The architecture of the TEG exhaust heat recovery system. (1,4 – Aluminum block; 2 – TEG module assembly; 3 – Compact heat exchanger housing; 5 – Diffuser).

Coolant water circulates through the flow fields inside the aluminum blocks to establish the temperature difference. TEG modules are assembled between the housing and the blocks.

Apart from part 5, the other four parts in Fig. 1 form the main body of the system. The size of the main body is determined by the number of TEG modules along and perpendicular to the flow direction, namely n_{run} and n_{cro}. These four parts are discretized into segments using a control volume methodology. As illustrated in Fig. 2, the segments are shaped via evenly dividing the whole system along and perpendicular to the flow direction by designated numbers, n_x and n_y. Each segment includes a part of TEG modules and the heat reservoirs on both sides.

Part 5 in Fig. 1 is the diffuser, the function of which is to distribute the exhaust gas homogeneously among the flow passages inside the heat exchanger housing. The exhaust gas is from a 1 kW HTPEMFC stack operating under normal conditions. The gas flow rate is $\dot{m}_{gas} = 12.61$ g/s. Its temperature is $t_{gas} = 148.2$ °C. Its humidity ratio is $\omega_{gas} = 0.02076$. Considering that the stoichiometry is as high as 20 and the oxygen depletion is small, it is of satisfactory accuracy to model the exhaust gas as ideal moist air. The thermodynamic data are from Hyland and Wexler [30]. The remaining assumptions of the numerical model are as follows:

1) There is no heat loss from the system to the surroundings.
2) The electrical/thermal contact resistances between the TEG modules and the electric load/heat reservoirs are neglected. There are no heat bypasses through the gaps between the TEG modules.

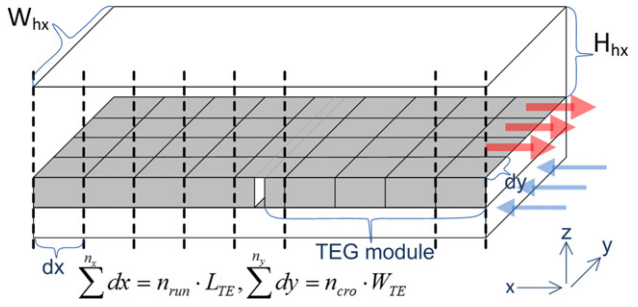

Fig. 2 – Control-volume scheme of the system.

3) Thermoelectric materials distribute homogeneously inside each module.
4) No phase change occurs inside the heat exchanger. Axial heat conduction is neglected. System performance is identical in the direction perpendicular to the exhaust gas flux.
5) When calculating the pressure drop, contraction and expansion pressure losses are neglected.
6) Heat conduction and convection in the aluminum blocks as well as between the TEG modules and the aluminum blocks are not taken into account. The coolant water flow is set to be high enough so a uniform temperature of 20 °C can represent the cold side.

Based on the above assumptions, the governing equations for each segment can be given based on the energy balance.

2.1. TEG modules

The way to model TEG modules is reconsidered compared to other publications in the field to better serve the system level study. Modules are treated as black boxes in the model. Inside each module, thermoelectric materials are supposed homogeneously distributed. Unlike most of the above literature, module parameters are from the experiments in [26], not directly substituted by material properties. Module performance calculated from empirical parameters is more reproducible in real-life applications. After the module is discretized in the x and y directions but not along the z axis, TEG performance is assumed uniform in each segment but vary with temperature between segments. For system design and fabrication, the advantage of modeling TEG modules in this way would be twofold: a) mitigating the model complexity and b) keeping the model precision from being affected by simplifying the details inside the TEG modules. The module parameters used in the current system are listed in Table 1. The Thomson effect is neglected because the temperature difference is relatively moderate in this case [31].

For each TEG segment, the corresponding energy balance is described by the following equations:

$$\dot{q}_{h,TE}(i) = (\overline{T}_{h,TE}(i) - \overline{T}_{c,TE}(i))/R_{t,i} + \alpha_i \overline{T}_{h,TE}(i) I_i - 0.5 I_i^2 R_{e,i}, \quad (1)$$

$$\dot{q}_{c,TE}(i) = (\overline{T}_{h,TE}(i) - \overline{T}_{c,TE}(i))/R_{t,i} + \alpha_i \overline{T}_{c,TE}(i) I_i + 0.5 I_i^2 R_{e,i}, \quad (2)$$

$$w(i) = \dot{q}_{h,TE}(i) - \dot{q}_{c,TE}(i). \quad (3)$$

All segments can either electrically work in series or in standalone mode. In standalone mode, the external ohmic resistance equals the internal when one segment reaches its peak power output and the corresponding electric current is:

$$I_i = 0.5(\alpha_i)(\overline{T}_{h,TE}(i) - \overline{T}_{c,TE}(i))/R_{e,i}. \quad (4)$$

The total power output of the whole TEG assembly can be summed up as:

$$P_{TEA} = \sum^{nx} \sum^{ny} w(i). \quad (5)$$

Table 1 – TEG module parameters [26].

Properties	Values
Type	Melcor HT8
$W_{TE} \cdot L_{TE}$ (m^2)	0.04001·0.04001
α_{TE} (V/K)	$-0.0000438 \cdot T_{av} + 0.05$
$R_{TE,e}$ (Ω)	$0.00638 \cdot T_{av} + 2.00$
$R_{TE,t}$ (K/W)	$0.000284 \cdot T_{av} + 1.54$

T_{av}–(°C), the average temperature between the two sides of each module.

2.2. Compact plate-fin heat exchanger

Choosing the best heat exchanger for heat recovery is a common problem. In the current model, a lookup table is integrated to alleviate this problem. The table contains 59 types of commercialized compact plate-fin heat exchangers. All the heat exchanger geometry and relevant parameters in the table are taken from [32]. Attempts towards numerical prediction of heat exchanger performance easily fail in matching experimental data. However the correlations and parameter data herein were generated from experimental work by Kays and London. These correlations and data have found extensive application in industry, particularly in less-critical designs. Compared to homemade heat exchanging structures, modeling in this way can better fulfill the system optimization and fabrication requests.

The governing equations to describe the heat transfer between the TEG assembly and the hot/cold fluids in each segment, respectively, are:

$$\dot{q}_{h,TE}(i) = \dot{q}_{gas}(i) = \dot{m}_{gas}(h_{gas,i} - h_{gas,i+1}), \quad (6)$$

$$\dot{q}_{gas}(i) = \varepsilon_{ctf}(i)\dot{m}_{gas}\left(h_{gas,i} - h_{gas,i}^{cw}\right), \quad (7)$$

$$\dot{q}_{h,TE}(i) = UA_{hx}(i)(\overline{T}_{gas}(i) - \overline{T}_{h,TE}(i)), \quad \overline{T}_{gas}(i) = (T_{gas}(i) + T_{gas}(i+1))/2. \quad (8)$$

The coefficients in the above functions are given as follows:

$$1/UA_{tot}(i) = 1/UA_{hx}(i) + 1/UA_{TE}(i), \quad (9)$$

$$\varepsilon_{ctf}(i) = 1 - \exp(-NTU(i)), \quad NTU(i) = 2UA_{tot}(i)\overline{T}_{gas}(i)/\dot{m}_{gas}(h_{gas,i} + h_{gas,i+1}). \quad (10)$$

h_{gas} is the enthalpy of the exhaust gas and h_{gas}^{cw} is the exhaust gas enthalpy at the temperature of the coolant water. They are calculated on each segment from functions found in [30]. $UA_{hx}(i)$ is the heat exchanger conductance in each segment, which describes both the air-exchanger heat convection and the heat conduction in the exchanger body. It is determined by the exchanger material and structure, the local fluid properties as well as the flow condition of the exhaust gas. In details, the key functions are [32]:

$$A_{hx}(i) = \tau(i) H_{hx} W_{hx} dx/n_y \quad (11)$$

$$Co(i) = j_{hx} u_{gas}(h_{gas,i} + h_{gas,i+1})/2Pr_i^{(2/3)}\overline{T}_{gas}(i) \quad (12)$$

$$u_{gas} = \dot{m}_{gas}/A_{ff} \quad (13)$$

$$RE_i = u_{gas} D_h/\nu_{gas,i} \quad (14)$$

For any kind of heat exchanger, there is an operational region of Reynolds number. This information is also available in the lookup table.

In addition, the pressure drop through the heat exchanger housing can be evaluated from the following function,

$$\Delta p_{hx} = \left(u_{gas}^2/\left(2\rho_{gas,in}\right)\right)\left[4f_{hx}L_{hx}\rho_{gas,in}/\left(D_h\bar{\rho}_{gas}\right) + (1+\sigma^2)\left(\left(\rho_{gas,in}/\rho_{gas,out}\right)-1\right)\right] \quad (15)$$

The Colburn factor j_{hx} and the Friction factor f_{hx} of plate-fin surfaces are also from the experimental source [32].

2.3. Solution methodology

The solution methodology of the numerical model is implemented by using a discretized ε-NTU approach [33]. Input parameters include the thermo-physical properties and electrical connection style of TEG modules, configuration parameters of TEG modules and plate-fin heat exchangers as well as the inlet exhaust gas parameters into the plate-fin heat exchanger. Then the fluid properties, thermoelectric performance and heat transfer process are updated on each segment along the flow direction. Finally, results are exported.

The discretized ε-NTU harnessed here is to make sure the model is better suited for both simulation-type and design-type problems [34]. Algebraically, it is identical with the log-mean temperature difference method (LMTD) [34].

3. Simulation results and discussion

In the following numerical simulation, the heat exchanger type used is called 'Strip-fin plate-fin, surface 1/4(s)-11.1' [35]. It is characterized by a low pressure drop for high heat exchanging capability [27]. More details of its specifications can be found in [32]. The only exception is in Section 3.5, where the performance of different heat exchangers is compared.

3.1. Model validation

A check is carried out to balance the computational requirements and the result accuracy. There are 10 Melcor HT8 modules along and perpendicular to the flow direction, under which case the system is oversized. All TEG segments during the simulation run are in standalone mode. In other words, each segment is assumed to be connected to a matched load to maximize its power output. According to the 4th assumption above, only the number of segments along the flow direction can potentially affect the simulation results. Therefore the segment number per TEG module is varied from 1 to 20 to observe its influence. The representative results of the TEG hot side temperature and the system power output are shown below.

In Fig. 3, it is clear that the effect of the number of segments on the TEG hot side temperature distribution is not significant. If this temperature distribution was studied independently, there would be no need to pay attention on the number of segments. On the other hand, it impacts the system power output evidently. Fig. 4 illustrates the system power output and its relative error versus the segment number. For a deviation less than 0.5%, cutting each module into 6 segments in the flow direction is the minimum requirement. It means it is not necessary to discretize each module by the width of each thermoelement or the distance between adjacent thermoelements as in literature. In the following simulations, this number is adjusted accordingly.

Simulations are then conducted to validate the system model with experimental data. Firstly, the discretized TEG model is compared with experimental results from [26]. Throughout the validation, three temperatures are respectively set to the module hot side, while the cold side is kept constant at 50 °C, to follow the experiment settings. Sorted by the temperature difference, the module power outputs are plotted in Fig. 5. The results show a perfect correspondence between the discretized TEG model and the experiments.

Secondly, the performance of the heat exchanger part is verified against the experimental results from [27]. The heat exchanger type harnessed in the experiments was also the one, 'Strip-fin plate-fin, surface 1/4(s)-11.1'. For comparison, the heat transferred and the pressure drop are used for comparison. Results are shown in Fig. 6.

According to Fig. 6, it can be concluded that the simulation results are in good agreement with the experimental results. They also show similar trends. The difference relatively observable only lies in the low flow rate region. The reason is that some vital details are missing in the reference, such as the exact temperature difference, the hot gas composition, among others. As a whole, the deviation still falls inside a 10% range. So it is concluded that the accuracy of the heat exchanger model is acceptable.

The numerical model of the TEG exhaust heat recovery system model is thus considered developed and validated. Before conducting optimization on the system configuration, a sensitivity analysis is essential to identify which parameters have more significant impact on the system performance.

3.2. Sensitivity analysis

A multiple parameter sensitivity analysis is carried out in this section to determine the main variables of this system that

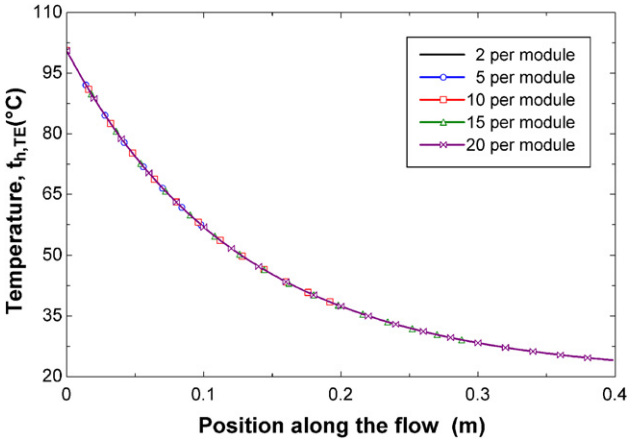

Fig. 3 – TEG hot side temperature distribution vs. the segment number.

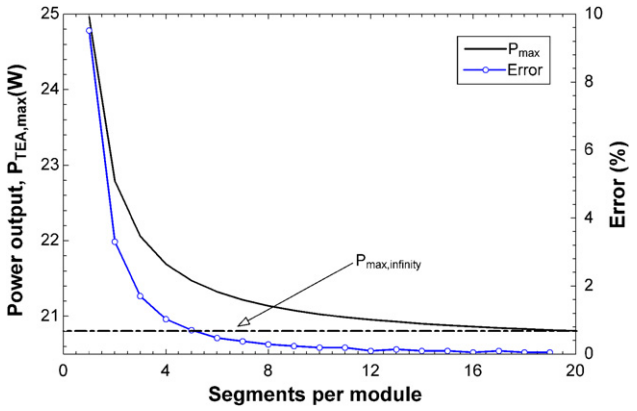

Fig. 4 – System power output with segments from 1 to 20 per module.

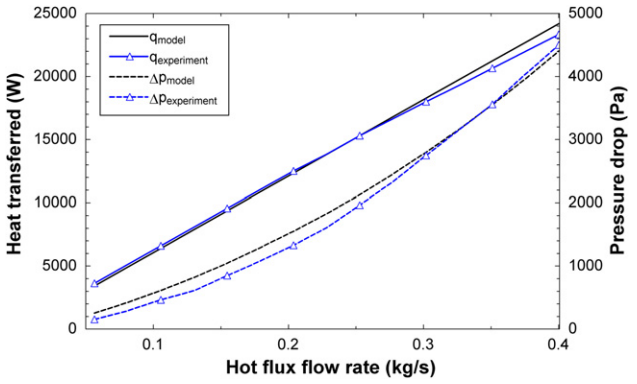

Fig. 6 – Heat exchanger model validation by heat transferred and pressure drop.

affect the performance. An uncertainty propagation tool is used to study the effects on system model output when the independent parameters vary in given ranges [35]. This method was initially designed for experiments to assess the deviations in measurement of the calculated variables. As described in [36], this calculation assumes the independent variables are uncorrelated and random, i.e. neglecting covariance between them; the uncertainty in the system performance can be expressed as

$$U_\eta = \sqrt{\sum_i (\partial\eta/\partial X_i)^2 U_{X_i}^2}, \text{ where } \eta = f(X_1, X_2, \ldots, X_n). \quad (16)$$

Here factors that affect the system power output $P_{TEA,max}$ and the heat exchanger pressure drop Δp_{hx} are analyzed using the uncertainty propagation. These factors can be distinguished into three categories: system structural parameters, TEG properties and operating conditions. System structural parameters further have two subcategories, namely system dimensions and heat exchanger type. Results are listed in Tables 2 and 3. Every input variable is set with a relative uncertainty of 5.00%.

The results show that the system power output and the pressure drop are affected by an uncertainty of 17.08% and 13.46%, respectively. The influences are rather significant, which means that some of the input parameters should be carefully treated in the simulation for higher model accuracy as well as in practice for better system performance.

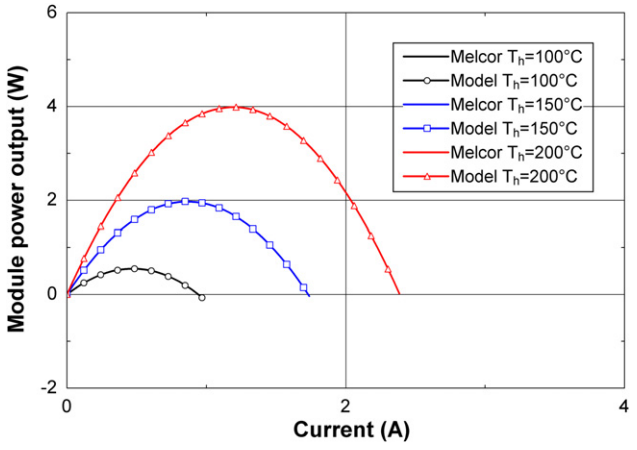

Fig. 5 – Validation of the discretized TEG model.

By observation it can be seen that the larger sources of the power output uncertainty are five parameters. These are the exhaust gas temperature, mass flow rate, specific heat, heat resistance of each TEG module and the module's Seebeck coefficient. As verified by many literatures, the exhaust gas temperature has extremely significant influence on the TEG power output. The exhaust gas temperature, together with the mass flow rate and the specific heat, determines the capacity of the heat source, which is available for TEGs to convert into electricity. Similarly, the module heat resistance and the Seebeck coefficient dominate the conversion efficiency of the whole TEG assembly. If any of the above parameters becomes larger, the system power output will increase and vice versa.

On the other hand some input parameters have negligible effect on the system power output. These include the exhaust gas pressure and most system structural parameters, such as the number of modules crossing the flow direction, number of modules along the flow direction and so on. The power output insensitivity to these structural parameters actually indicates that the current system is oversized. This insensitivity is also the side effect of all TEG segments working in standalone mode in the current system. The structural parameters will be more thoroughly analyzed in the following sections. Another parameter with little effect is the exhaust gas pressure. This can have a positive effect on the system electrical efficiency because little pressure boost is required for the recovery system. This can also simplify the connection between the recovery system and the fuel cell stack, because the feed gas pressure also has a minor effect on the fuel cell performance. As a whole, the system parasitic losses are decreased.

Parasitic losses and system pressure drops are roughly proportional in the current system. From Table 3, it can be concluded that almost all the uncertainty of the pressure drop comes out of the system structural parameters and the exhaust gas magnitude. Among them, the exhaust gas flow rate and number of TEG modules perpendicular to the flow have the most significant effect. The influence of the exhaust gas pressure, the height of the heat exchanger and number of TEG modules along the flow direction is also rather significant. These influences have been clearly described by the above Eq.

Table 2 – Sensitivity study on system power output.

Input parameters and description		Value	Uncertainty contribution (%)
$A_{fin\backslash A}$	Fin area/total area	0.756	−0.00
α_{hx}	Heat transfer area/total volume (m^2/m^3)	915.6	1.35
H_{hx}	Height of heat exchanger (m)	0.00635	0.71
fin_{thk}	Thickness of fins (not applicable to pin-fin) (m)	0.000152	0.00
$Co_{hx,av}$	The exchanger average heat conductivity (W/m^2-K)	80.58	1.30
n_{cro}	Number of modules cross the flow direction	10	0.01
n_{run}	Number of modules along the flow direction	10	0.01
α_{TE}	Seebeck coefficient of each TEG module (V/K)	0.05	19.67
$R_{TE,e}$	Electric resistance of each TEG module (Ω)	2	−4.92
$R_{TE,t}$	Heat resistance of each TEG module (K/W)	1.54	10.71
$\dot{m}_{gas}$	The exhaust gas mass flow rate (kg/s)	0.01261	7.96
Cp_{gas}	Average exhaust gas specific heat (J/kg-°C)	1047	7.96
ω_{gas}	Humidity Ratio	0.02076	−0.00
p_{gas}	Gas pressure (Pa)	1	0.00
t_{gas}	Gas temperature (°C)	148.2	44.51
t_{cw}	Coolant water temperature (°C)	20	−0.89
Output	Variable description	Value	Uncertainty (%)
$P_{TEA,max}$	Maximum power output of the system	24.10 (W)	± 4.12 (W) (±17.08%)

(15). On the contrary, the effect of the exhaust gas temperature and its specific heat is relatively moderate. It can be noticed that, even in the current oversized system, the system structural parameters still have dramatic impact on the system pressure drop. To lower the pressure drop, as well as maximize the system net power output, the system dimensions and the heat exchanger types need a more detailed analysis.

3.3. *Influence of* n_{cro}

The number of TEG modules perpendicular to the flow direction is varied to investigate the impact of the heat exchanger width on the system power output and the pressure drop. All TEG segments in this study worked in standalone mode. The number of TEG modules along the flow direction was designated to 30. Under this condition the system was always oversized along the flow direction for every n_{cro}. In the simulation, n_{cro} increased from the minimum value of 2. Under the above settings, the system power output will reach its upper limit in all cases.

The simulation results are shown in Fig. 7. The width tends to decrease the electric power generated and the pressure drop simultaneously. The pressure drop falls sharply down in the beginning. But after n_{cro} reaches 8, the effect is rather moderate. On the other hand the system power output drops gradually all the way down with n_{cro} increasing, although a little bit faster in the first half range. The increasing width increases the cross section area of the flow passage. The flow speed then drops. In turn, it can be calculated by Eq. (15) that the pressure drop will decrease. But with decreasing flow speed, Reynolds number is also becoming smaller. As a result, poorer convective heat transfer in the heat exchanger will reduce the temperature difference on TEG modules and reduce the power output.

Table 3 – Sensitivity study on the system pressure drop.

Input parameters and description		Value	Uncertainty contribution (%)
$A_{fin\backslash A}$	Fin area/total area	0.756	0.00
α_{hx}	Heat transfer area/total volume (m^2/m^3)	915.6	−0.00
H_{hx}	Height of heat exchanger (m)	0.00635	−15.64
fin_{thk}	Thickness of fins (not applicable to pin-fin) (m)	0.000152	−0.00
$Co_{hx,av}$	The exchanger average heat conductivity (W/m^2-K)	80.58	−0.00
n_{cro}	Number of modules cross the flow direction	10	−28.11
n_{run}	Number of modules along the flow direction	10	13.13
α_{TE}	Seebeck coefficient of each TEG module (V/K)	0.05	0.00
$R_{TE,e}$	Electric resistance of each TEG module (Ω)	2	0.00
$R_{TE,t}$	Heat resistance of each TEG module (K/W)	1.54	0.01
$\dot{m}_{gas}$	The exhaust gas mass flow rate (kg/s)	0.01261	28.06
Cp_{gas}	Average exhaust gas specific heat (J/kg-°C)	1047	0.03
ω_{gas}	Humidity Ratio	0.02076	−0.00
p_{gas}	Gas pressure (Pa)	1	−13.80
t_{gas}	Gas temperature (°C)	148.2	1.20
t_{cw}	Coolant water temperature (°C)	20	0.02
Output	Variable description	Value	Uncertainty (%)
Δp_{hx}	Pressure drop of the system	383.10 (Pa)	± 51.58 (Pa) (±13.46%)

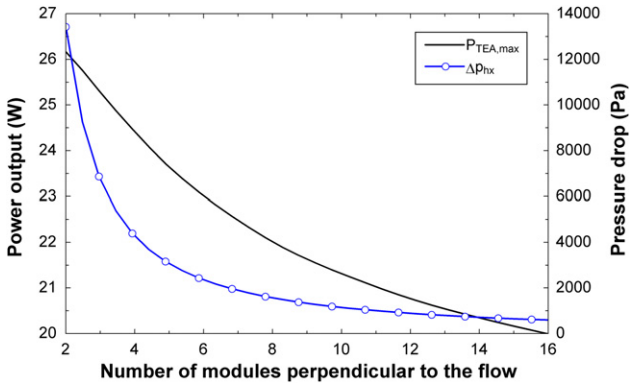

Fig. 7 – Power output and pressure drop vs. number of TEG modules cross the gas flow.

As mentioned above, the pressure drop accounts for most of the system parasitic losses, through determining the power demand of the blower in the system. If only the following function from [37] is used to assess the power demand, an n_{cro} value higher than 8 will be the preferred choice. But actually, the blower in the whole fuel cell and TEG integrated system mainly serves the fuel cell stack. Therefore a further systematic study is essential here to more properly predict the effect of the recovery system pressure drop on the net power output of the whole system. In this paper, the value of n_{cro} is set to 6 in the following analysis.

$$P_{comp} = \dot{m}_{gas} R_{gas} T_{in} \ln(p_{out}/p_{in}) / M_{gas} \eta_{comp} \quad (17)$$

3.4. *Influence of* n_{run}

A simulation was also carried out to study the effect on the system performance from the length of the flow channels, which is determined by the number of TEG modules along the exhaust gas flow direction, n_{run}. The other settings were: n_{cro} was fixed to 6; all TEG segments were either in series or in standalone mode. The results are compared in Fig. 8.

It can be seen that the two system power output curves are overlapped and increase very fast in the beginning. Then the power output curve, when all TEG segments are operating in standalone mode, tends to approach the theoretical upper limit. There is no optimum value of n_{run}. But the power output of all segments in series starts to drop down slowly after reaching the maximum point, where $n_{run} = 7$. This effect is similar as what has been reported in [38]. It was believed that the peak point is the trade-off between the electromotive force and the internal resistance, when all TEG modules are in series. In real-life applications, both of the above connection methods of the TEG segments are either lacking feasibility or reliability. A mixed connection method and an intermediate power output are considered more feasible.

On the other hand the system pressure drop under both connection conditions is roughly proportional to n_{run} in the whole range. It can also be noticed that the two curves are completely overlapping. This phenomenon corresponds with the above sensitivity analysis, which proved that the system pressure drop is independent from the performance of the TEG modules.

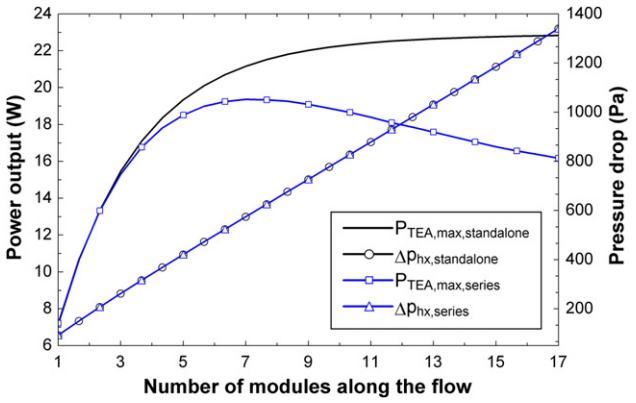

Fig. 8 – Power output and pressure drop vs. n_{run}.

3.5. *Influence of heat exchanger design*

In this section, different types of heat exchangers are compared by the influence on the system power output and the pressure drop. Based on the analyses above, 6 TEG modules were aligned across the exhaust gas flow in the simulation; 7 modules were along the flow direction. All TEG segments were electrically connected in standalone mode. Judged by their feasible Reynolds number interval, the results from 33 types of plate-fin heat exchangers among all 59 types are shown in Fig. 9. The results are sorted by the power output. Heat exchangers with pressure drop larger than 900 Pa are not included.

It can be seen that with the ascending power output, the pressure drop fluctuates significantly between different heat exchangers. Obviously, heat exchangers with higher power output and lower pressure drop are superior. From Fig. 9, four types are identified of interest for further study, namely 'Plain plate-fin, surface 15.08' (17), 'Pin-fin plate-fin, surface PF-10(F)' (25), 'Strip-fin plate-fin, surface 1/6–12.18(D)' (28) as well as 'Pin-fin plate-fin, surface PF-4(F)' (33). The type 'Strip-fin plate-fin, surface 1/4(s)-11.1' currently used in the exhaust heat recovery system is the type (19) in Fig. 9.

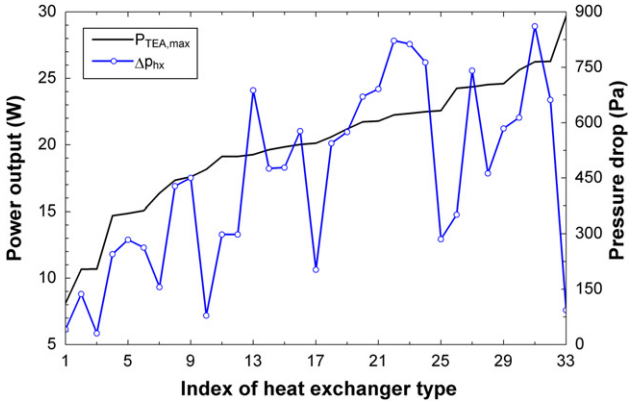

Fig. 9 – Power output and pressure drop using different heat exchangers.

4. Conclusions

A numerical model of a TEG heat recovery system for the exhaust gas from a HTPEMFC stack was developed. It is based on a finite-element approach with more precisely described gas properties and heat transfer. For both design-type and simulation-type problems, the versatility of the model is enhanced by the integrated database of 59 types of plate-fin heat exchangers and the discretized ε-NTU solution method. In summary, the model can help optimize the system design and operation with higher accuracy and flexibility. In turn, this can benefit the system fabrication.

A sensitivity analysis was then carried out on the system model. It is found that exhaust gas parameters and heat exchanger structure have a significant effect on the system power output and the pressure drop. Gas properties should be precisely described. The configuration of the system should be carefully optimized to maximize its performance.

Based on the model, the optimized system configuration of the heat recovery system is finally depicted. There are 6 TEG modules crossing the exhaust gas flow and 7 modules along the flow. In the system, the TEG module type is assumed to be the Melcor HT8 type. They are all electrically connected in series. The heat exchanger, type 'Strip-fin plate-fin, surface 1/4(s)-11.1', is implemented, which was also chosen by other researchers [27].

Screening the whole database of different heat exchangers, it turns out that the heat exchanger structure currently used in the system is probably not the best choice; Four other types are identified with superior performance and worthy of further analysis.

Future work is needed; Experiments are still needed to verify the model accuracy. The heat transfer phenomena in the coolant water side and water vapor phase change in the exhaust gas could be included to improve the model robustness. In the sensitivity analysis, uncertainty intervals of the input parameters need further consideration to better reflect realistic conditions. In comparing different heat exchangers, the system dimensions will be optimized for them respectively. More types of heat exchangers can also be included in the database.

Acknowledgments

The authors gratefully acknowledge financial support from Aalborg University and China Scholarship Council. The authors would like to thank Alexandros Arsalis for reviewing.

REFERENCES

[1] Wang Y, Chen KS, Mishler J, Cho SC, Adroher XC. A review of polymer electrolyte membrane fuel cells: technology, applications, and needs on fundamental research. Applied Energy 2011;88(4):981–1007.

[2] Andreasen SJ, Ashwortha L, Remóna INM, Kær SK. Directly connected series coupled HTPEM fuel cell stacks to a Li-ion battery DC-bus for a fuel cell electrical vehicle. International Journal of Hydrogen Energy 2008;33(23): 7137–45.

[3] Rowe DM. Thermoelectric generators as alternative sources of low power. Renewable Energy 1994;5(2):1470–8.

[4] Crane DT, LaGrandeur JW. Progress report on BSST-Led US department of energy automotive waste heat recovery program. Journal of Electronic Materials 2010;39(9):2142–248.

[5] Auckland DW, Shuttleworth R, Luff AC, Axcell BP, Rahman M. Design of a semiconductor thermoelectric generator for remote subsea wellheads. Electric Power Applications, IEE Proceedings 1999;142(2):65–70.

[6] Yang J, Stabler FR. Automotive applications of thermoelectric materials. Journal of Electronic Materials 2009;38(7):1245–51.

[7] Chen M, Sasaki Y, Suzuki RO. Computational modeling of thermoelectric generators in marine power plants. Materials Transactions 2011;52(8):1549–52.

[8] Snyder GJ, Toberer ES. Complex thermoelectric materials. Nature Materials 2008;7(2):105–14.

[9] Minnich AJ, Dresselhaus MS, Ren ZF, Chen G. Bulk nanostructured thermoelectric materials: current research and future prospects. Energy & Environmental Science 2009; 2(5):466–79.

[10] Venkatasubramanian R, Siivola E, Colpitts T, O'Quinn B. Thin-film thermoelectric devices with high room-temperature figures of merit. Nature 2001;413(6856):597–602.

[11] Gao M, Rowe DM. Ring-structured thermoelectric module. Semiconductor Science and Technology 2007; 22(8):880–3.

[12] Bell LE. Cooling, heating, generating power, and recovering waste heat with thermoelectric systems. Science 2008; 321(5895):1457–61.

[13] Chen M, Lund H, Rosendahl L, Condra T. Energy efficiency analysis and impact evaluation of the application of thermoelectric power cycle to today's CHP systems. Applied Energy 2010;87(4):1231–8.

[14] Ioffe AF. Semiconductor thermoelements and thermoelectric cooling. London: Infoseach Limited; 1957.

[15] Rowe DM, Gao M. Evaluation of thermoelectric modules for power generation. Journal of Power Sources 1998;73(2):193–8.

[16] Crane D, Bell LE. Progress towards maximizing the performance of a thermoelectric power generator. In: Proceedings of International Conference on thermoelectrics, vol. 1; 2006. p. 11–6.

[17] Chen M, Rosendahl LA, Condra T. A three-dimensional numerical model of thermoelectric generators in fluid power systems. International Journal of Heat and Mass Transfer 2011;54(1–3):345–55.

[18] Hendricks TJ, Lustbader JA. Advanced thermoelectric power system investigations for light-duty and heavy duty applications: part II. In: Proceedings of the 21st International Conference on thermoelectrics, vol. 1; 2002. p. 381–94.

[19] Chen J, Wu C. Analysis on the performance of a thermoelectric generator. Journal of Energy Resources Technology 2000;122(2):61–3.

[20] Esartea J, Gao M, Rowe DM. Modelling heat exchangers for thermoelectric generators. Journal of Power Sources 2001; 93(1–2):72–6.

[21] Pramanick AK, Das PK. Constructal design of a thermoelectric device. International Journal of Heat and Mass Transfer 2006;49(7–8):1420–9.

[22] Suzuki RO, Tanaka D. Mathematical simulation of thermoelectric power generation with the multi-panels. Journal of Power Sources 2003;122(2):201–9.

[23] Suzuki RO, Tanaka D. Mathematic simulation on thermoelectric power generation with cylindrical multi-tubes. Journal of Power Sources 2003;124(1):293–8.

[24] Crane DT, Jackson GS. Optimization of cross flow heat exchangers for thermoelectric waste heat recovery. Energy Conversion and Management 2004;45(9–10):1565–82.

[25] Yu J, Zhao H. A numerical model for thermoelectric generator with the parallel-plate heat exchanger. Journal of Power Sources 2007;172(1):428–34.
[26] Smith KD. An investigation into the viability of heat sources for thermoelectric power generation systems, [Master thesis]. Rochester (NY): Rochester Institute of technology; 2009.
[27] Espinosa N, Lazard M, Aixala L, Scherrer H. Modeling a thermoelectric generator applied to diesel automotive heat recovery. Journal of Electronic Materials 2010;39(9):1446–55.
[28] Chen M, Andreasen SJ, Rosendahl L, Kær SK, Condra T. System modeling and validation of a thermoelectric fluidic power source: PEMFC-TEG. Journal of Electronic Materials 2010;39(9):1593–600.
[29] Chen X, Pan Y, Chen J. Performance and evaluation of a fuel cell – thermoelectric generator hybrid system. Fuel Cells 2010;10(6):1164–70.
[30] Hyland RW, Wexler A. Formulations for the thermodynamic properties of the saturated phases of H_2O from 173.15 K to 473.15 K. ASHRAE Transactions 1983;89(2A):500–19.
[31] Lazard M, Fraisse G, Goupil C, Scherrer H. Thermal analysis of a thermoelectric: a way to non conventional design. In: Proceedings of the 6th European Conference on thermoelectrics, vol. 1; 2008. p. 2–15.
[32] Kays WM, London AL. Compact heat exchangers. 3rd ed. New York: McGraw Hill; 1984.
[33] Iu I, Weber NA, Bansal P, Fisher DE. Applying the effectiveness-NTU method to elemental heat exchanger models. ASHRAE Transactions 2007;113(1):504–13.
[34] Nellis G, Klein S. Heat transfer. New York: Cambridge University Press; 2009.
[35] F-Chart Software. EES manual, www.fchart.com; 2010. v8.590 Edition.
[36] Taylor BN, Kuyatt CE. Guidelines for evaluating and expressing the uncertainty of NIST measurement results. National Institute of Standards and Technology; 1994 [Technical Note 1297].
[37] Kolb G. Fuel processing: for fuel cells. Weinheim, Germany: Wiley-VCH; 2008.
[38] Mori M, Yamagami T, Oda N, Hattori M, Sorazawa M, Haraguchi T. Current possibilities of thermoelectric technology relative to fuel economy. Society of Automotive Engineering; 2009. 2009-2101–0170.

Nomenclature

A_{ff}: minimum free flow area, m^2
A_{hx}: total heat transfer area, m^2
c: gas specific heat, J/kg-K
D_h: hydraulic diameter, m
f_{hx}: Friction factor
h: exhaust gas enthalpy, kJ/kg
H: component height, m
I: electric current, A
j_{hx}: Colburn factor
L: component length, m
n_x: total number of segments along the flow
n_y: total number of segments crossing the flow
P: power output or consumption, W
Δp: pressure drop, Pa
q: heat transferred, W
T, t: temperature, K, °C
u_{gas}: core mass velocity, Kg/s-m^2
w: power output of each segment, W
W: component width, m

Greek symbols

ε_{ctf}: the effectiveness
ν: kinematic viscosity, m^2/s
ρ: exhaust gas density, kg/m^3
σ: minimum free flow area/frontal area
τ: heat transfer area/exchanger volume, 1/m

Subscripts/Superscripts

c,TE: cold side of the TEG module
cw: coolant water
e: electrical resistance
gas: exhaust gas
h,TE: hot side of the TEG module
hx: heat exchanger
i: segment index
max: maximum value
t: thermal resistance
TEA: whole TEG assembly

Abbreviation

Co: exchanger heat conductivity, W/m^2-K
NTU: number of transfer units
Pr: Prandtl number
RE: Reynolds number
UA: heat exchanger conductance, W/K
ZT: nondimensional figure-of-merit of module